ISSN 1948-9358 (online)

World Journal of *Diabetes*

World J Diabetes 2024 September 15; 15(9): 1829-2001

Published by Baishideng Publishing Group Inc

World Journal of Diabetes

Contents

Monthly Volume 15 Number 9 September 15, 2024

EDITORIAL

FIELD OF VISION

REVIEW

MINIREVIEWS

ORIGINAL ARTICLE

Case Control Study

World Journal of Diabetes

Monthly Volume 15 Number 9 September 15, 2024

Contents

World Journal of Diabetes

Monthly Volume 15 Number 9 September 15, 2024

Contents

NAME OF JOURNAL
World Journal of Diabetes

ISSN
ISSN 1948-9358 (online)

LAUNCH DATE
June 15, 2010

FREQUENCY
Monthly

EDITORS-IN-CHIEF
Lu Cai, Md. Shahidul Islam, Michael Horowitz

EDITORIAL BOARD MEMBERS
https://www.wjgnet.com/1948-9358/editorialboard.htm

PUBLICATION DATE
September 15, 2024

INSTRUCTIONS TO AUTHORS
https://www.wjgnet.com/bpg/gerinfo/204

GUIDELINES FOR ETHICS DOCUMENTS
https://www.wjgnet.com/bpg/GerInfo/287

GUIDELINES FOR NON-NATIVE SPEAKERS OF ENGLISH
https://www.wjgnet.com/bpg/gerinfo/240

PUBLICATION ETHICS
https://www.wjgnet.com/bpg/GerInfo/288

PUBLICATION MISCONDUCT
https://www.wjgnet.com/bpg/gerinfo/208

ARTICLE PROCESSING CHARGE
https://www.wjgnet.com/bpg/gerinfo/242

STEPS FOR SUBMITTING MANUSCRIPTS
https://www.wjgnet.com/bpg/GerInfo/239

ONLINE SUBMISSION
https://www.f6publishing.com

World Journal of Diabetes

Submit a Manuscript: https://www.f6publishing.com

World J Diabetes 2024 September 15; 15(9): 1962-1978

DOI: 10.4239/wjd.v15.i9.1962

ISSN 1948-9358 (online)

ORIGINAL ARTICLE

Basic Study

Dexmedetomidine ameliorates diabetic intestinal injury by promoting the polarization of M2 macrophages through the MMP23B pathway

Man Lu, Xiao-Wen Guo, Fang-Fang Zhang, Dan-Hong Wu, Di Xie, Feng-Qin Luo

Specialty type: Endocrinology and metabolism

Provenance and peer review: Unsolicited article; Externally peer reviewed.

Peer-review model: Single blind

Peer-review report's classification

Scientific Quality: Grade B, Grade B, Grade C, Grade C

Novelty: Grade B, Grade B

Creativity or Innovation: Grade B, Grade C

Scientific Significance: Grade B, Grade B

P-Reviewer: Barbalho SM; Dąbrowski M; Horowitz M; Sahu SK

Received: June 5, 2024

Revised: July 17, 2024

Accepted: August 12, 2024

Published online: September 15, 2024

Processing time: 83 Days and 3.3 Hours

Man Lu, Xiao-Wen Guo, Fang-Fang Zhang, Dan-Hong Wu, Feng-Qin Luo, Department of Anesthesiology, The First Affiliated Hospital of Zhejiang Chinese Medical University (Zhejiang Provincial Hospital of Traditional Chinese Medicine), Hangzhou 310006, Zhejiang Province, China

Di Xie, Department of Emergency, Xinhua Hospital Affiliated to Shanghai Jiao Tong University School of Medicine, Shanghai 200092, China

Corresponding author: Feng-Qin Luo, MM, Attending Doctor, Department of Anesthesiology, The First Affiliated Hospital of Zhejiang Chinese Medical University (Zhejiang Provincial Hospital of Traditional Chinese Medicine), No. 54 Youdian Lane, Shangcheng District, Hangzhou 310006, Zhejiang Province, China. 3021702500@qq.com

Abstract

BACKGROUND

Diabetes is often associated with gastrointestinal dysfunctions, which can lead to hypoglycemia. Dexmedetomidine (DEX) is a commonly used sedative in perioperative diabetic patients and may affect gastrointestinal function.

AIM

To investigate whether sedative doses of DEX alleviate diabetes-caused intestinal dysfunction.

METHODS

Sedation/anesthesia scores and vital signs of streptozotocin (STZ)-induced diabetic mice under DEX sedation were observed. Diabetic mice were divided into saline and DEX groups. After injecting sedatives intraperitoneally, tight junctions (TJs) and apoptotic levels were evaluated 24 hours later to assess the intestinal barrier function. The role of DEX was validated using Villin-MMP23B flox/flox mice with intestinal epithelial deletion. *In vitro*, high glucose and hyperosmolarity were used to culture Caco-2 monolayer cells with STZ intervention. Immunofluorescence techniques were used to monitor the barrier and mitochondrial functions.

RESULTS

MMP23B protein levels in the intestinal tissue of STZ-induced diabetic mice were significantly higher than those in the intestinal tissue of control mice, with the DEX group displaying decreased MMP23B levels. Diabetes-mediated TJ dis-

ruption, increased intestinal mucosal permeability, and systemic inflammation in wild-type mice might be reversed by DEX. In Caco-2 cells, MMP23B was associated with increased reactive oxygen species accumulation, mitochondrial membrane potential depolarization, and TJ disruption.

CONCLUSION
DEX reduces MMP23B, which may potentially contribute to STZ-induced intestinal barrier dysfunction, affecting TJ modification through mitochondrial dysfunction.

Key Words: Diabetes; Dexmedetomidine; Intestinal barrier; Piezo1; Tight junctions

Core Tip: This study investigates the protective role of dexmedetomidine (DEX) in diabetic intestinal injury through the MMP23B pathway. The findings reveal that DEX acts as a sedative and enhances intestinal barrier function by promoting M2 macrophage polarization and reducing mitochondrial dysfunction. Streptozotocin-induced diabetic mice and Caco-2 cell models provide robust evidence of the potential therapeutic benefits of DEX, offering insights into its dual functionality in managing sedation and intestinal healing under diabetic conditions. This research can pave the way for the development of new treatment strategies targeting intestinal complications in diabetic patients.

Citation: Lu M, Guo XW, Zhang FF, Wu DH, Xie D, Luo FQ. Dexmedetomidine ameliorates diabetic intestinal injury by promoting the polarization of M2 macrophages through the MMP23B pathway. *World J Diabetes* 2024; 15(9): 1962-1978
URL: https://www.wjgnet.com/1948-9358/full/v15/i9/1962.htm
DOI: https://dx.doi.org/10.4239/wjd.v15.i9.1962

INTRODUCTION

Type 2 diabetes mellitus (T2DM) is a multifactorial disease characterized by tissue-specific dysregulation, and a complex interplay of genetic and environmental factors contribute to its pathogenesis[1-3]. Although the endocrine aspects of T2DM have been extensively studied, its intestinal component remains poorly explored. The gut, often overlooked, plays a pivotal role in glucose homeostasis and may be a key intervention area.

Intestinal macrophages are key players involved in the homeostasis of the gastrointestinal tract, performing several functions including supporting intestinal neurons, facilitating gastrointestinal motility, participating in oral tolerance to food antigens, and contributing to pathogen clearance. However, intestinal macrophages are also implicated in T2DM pathogenesis. Emerging evidence suggests that alterations in the functional profile of intestinal macrophages can incite metabolic inflammation, thereby accelerating obesity and T2DM progression[4-6].

T2DM can lead to gastrointestinal motility disorders, such as decreased gastric motility. However, the specific mechanisms linking T2DM to these gastrointestinal changes are not fully elucidated. Anesthetics, including dexmedetomidine (DEX), influence various physiological processes, but their impact on intestinal macrophages in diabetic contexts remains poorly understood.

DEX, a selective alpha-2 adrenergic receptor agonist, is widely used for its sedative, analgesic, and anxiolytic properties. In the context of infection and other pathological conditions, DEX enhances intestinal microcirculation, alleviates postoperative pain, and decreases opioid requirements[7-12]. Given its potential influence on inflammatory and immune responses, DEX may modulate the activity of intestinal macrophages, affecting T2DM-associated gastrointestinal dysfunctions.

In the present study, we aimed to delineate the intricate relationship between macrophages and DEX in the context of T2DM. By establishing a streptozotocin (STZ)-induced diabetic mouse model, we investigated the role of DEX in diabetes-induced gastrointestinal injury through comprehensive *in vivo* and *in vitro* experiments. Understanding the interaction between DEX and intestinal macrophages can unveil novel mechanisms underlying diabetes-related gastrointestinal complications and identify targets for therapeutic intervention. Our findings provide a fresh perspective on the intricate dynamics of diabetes-related intestinal dysfunction and may pave the way for the development of innovative treatment strategies that leverage the pharmacological potential of DEX to modulate macrophage activity and ameliorate gastrointestinal disturbances in diabetic patients.

MATERIALS AND METHODS

Analysis of the GSE63992 dataset

Differential gene analysis was performed on data sourced from the Gene Expression Omnibus database GSE63992. Volcano plots and heatmaps were generated, and R language packages were used for data processing[7,8].

Gene set enrichment analysis

A Gene Ontology/Kyoto Encyclopedia of Genes and Genomes (KEGG) analysis was performed on the data sourced from the Gene Expression Omnibus database GSE63992. R language packages were applied for data processing, and the corresponding bubble, circular, and bar charts, which also facilitated the analysis of gene overlaps within the identified Gene Ontology terms, were obtained. Furthermore, the involvement of differentially expressed genes (DEGs) in specific pathways was analyzed using DAVID[9,10].

Identification of hub genes

Gene networks were visualized using Cytoscape 3.6.1, and further analyzed within the STRING database to investigate biological processes.

Mice

Villin-CreERT, MMP23B flox/flox, and wild-type (WT) C57BL/6 male mice aged 6-8 weeks were provided by the Xinhua Hospital affiliated with the Shanghai Jiao Tong University School of Medicine. All animals were handled according to the 3R principle and in compliance with animal welfare standards.

Diabetic mouse model

The mice were divided into the following groups: Control, diabetes (DB), DB + MMP23B knockout (KO), DEX + DB, and DEX. The DB and DEX + DB mice were injected with STZ (40 mg/kg, intraperitoneal) daily for 5 days[11,12].

Macrophage depletion

We used clodronate liposomes (Cls), which are taken up by macrophages through endocytosis; the release of clodronate by lysosomes induces apoptosis and depletes macrophages. Mice were randomly assigned to one of the following four groups: Sham + phosphate buffered saline (PBS) (Sham; n = 4), DB (n = 4), MMP23B KO + DB + Cls (MMDC; n = 4), and MMP23B KO + PBS (MMP; n = 4). Cls or control (PBS) were intraperitoneally administered at a 24-hour interval before the DB procedure[13,14].

Caco-2 cell culture and treatment

We obtained Caco-2 cells from the Cell Bank of the Chinese Academy of Sciences, and four groups were randomly assigned: PBS (n = 4), MMP23B (n = 4), MMP23B + GM6001 (n = 4).

Immunofluorescence

Immunofluorescence staining was performed on frozen and paraffin tissue sections. Cells and tissues were fixed on glass slides or centrifuge tubes using 4% paraformaldehyde to preserve their morphological structure and protein distribution. Samples were treated with 0.1% Triton X-100 to increase antibody entry and binding. Nonspecific binding sites were blocked by adding an appropriate concentration of bovine serum albumin. Specific antibodies targeting the proteins of interest [CD 86 (AiFang, AF16377, 1:1000, rabbit polyclonal IgG), ZO-1 (Santa Cruz, sc-33725, 1:100, rat monoclonal IgG), and occludin (Santa Cruz, sc-133256, 1:100, mouse monoclonal IgG)] were added, and samples were incubated overnight at 4 °C. Secondary antibodies labeled with specific dyes [FITC-labeled donkey anti-rabbit IgG (Servicebio, GB22403, 1:200) and Cy3-labeled goat anti-mouse IgG (Servicebio, GB21303, 1:200)] were used for fluorescent signal detection. Samples were washed several times with a buffer solution to remove unbound secondary antibodies and other nonspecifically binding molecules. Slides were placed under a fluorescence microscope, and fluorescent signals were observed, detected, and recorded after illuminating with a specific wavelength. All images were captured using an Olympus fluorescence microscope (Olympus, BX53)[15,16].

Enzyme-linked immunosorbent assay

Samples (tissue extracts) were collected and diluted or processed as needed. The target molecule was dissolved in a buffer solution and added to the wells of an enzyme-linked immunosorbent assay plate. The solid phase was allowed to interact with the target molecule, and the plate was incubated at room temperature or under refrigerated conditions. This step allows the target molecule to adsorb onto the solid phase[17].

Mitochondrial membrane potential measurement

The mitochondrial membrane potential (ΔΨm) was determined according to the manufacturer's instructions. After washing the cells, a JC-1 working solution was labeled for 20 minutes (37 °C). The dual fluorescence imaging of JC-1 was completed using a RuoChuang camera[18]. Using the JC-1 monomer level to assess mitochondrial health is of great significance as it can reflect changes in ΔΨm. ΔΨm is an important indicator of mitochondrial function, and its decrease is usually associated with early apoptosis events. As a fluorescent probe, JC-1 can exhibit different fluorescent properties under different ΔΨm states. When ΔΨm is high, JC-1 is in a polymeric form inside the mitochondria, emitting red fluorescence; however, when ΔΨm decreases, JC-1 exists in a monomeric form in the cytoplasm, emitting green fluorescence. This change in fluorescence color provides an intuitive and sensitive method for detecting ΔΨm.

In research on diabetic intestinal injury, a specific detection method using JC-1 can help reveal changes in mitochondrial function under diabetic conditions. Diabetes may lead to mitochondrial dysfunction, including decreased ΔΨm, thereby affecting the energy metabolism of intestinal cells and cell apoptosis. Through JC-1 detection, researchers can observe changes in ΔΨm of intestinal cells in a diabetic mouse model and further explore the impact of diabetes on

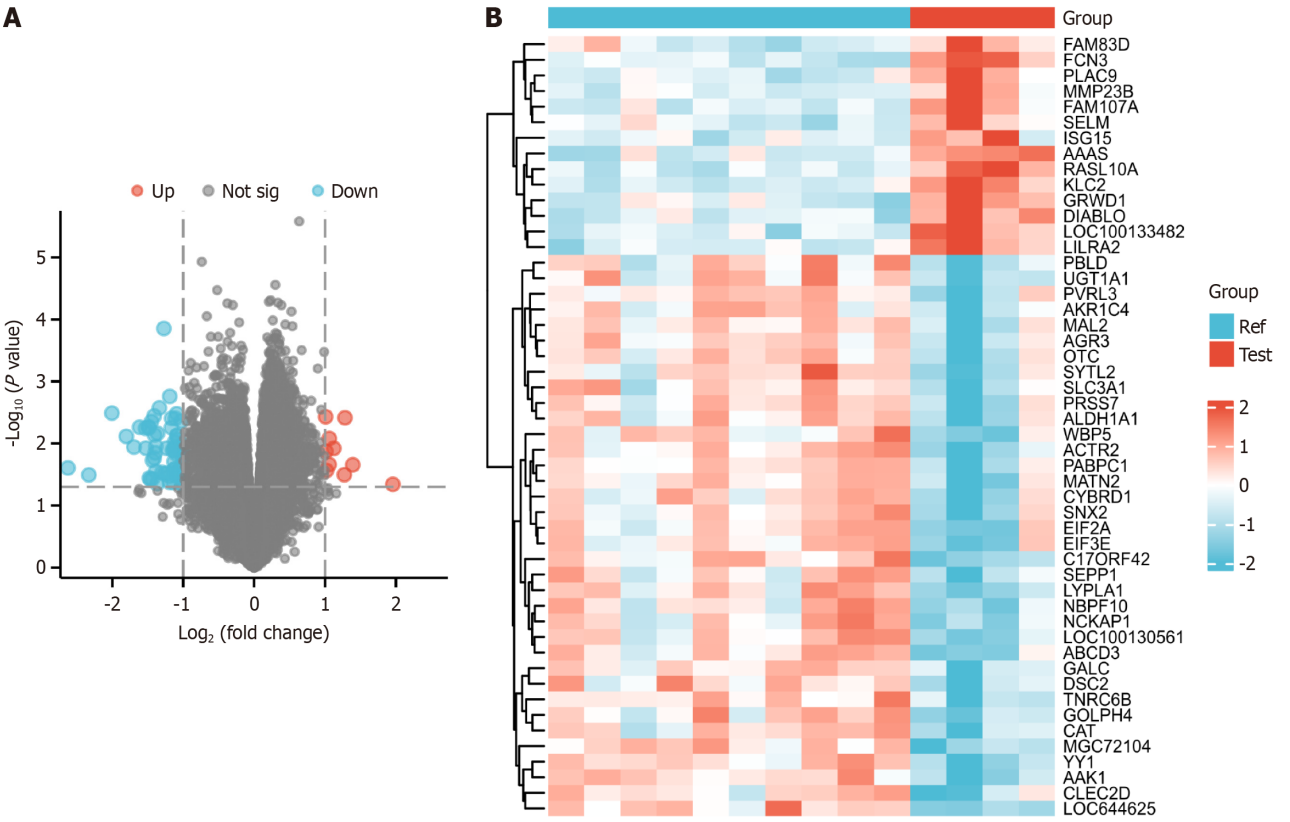

Figure 1 Data processing and differentially expressed gene identification. A: Heatmap of sample-to-sample correlation. The diabetes group displayed a stronger intragroup correlation than the control group; B: Volcano plot generated using the limma R tool, showcasing all differentially expressed genes in the control and diabetes groups.

mitochondrial function in intestinal cells.

Furthermore, the versatility of the JC-1 staining method makes it suitable for various cell types, including muscle cells and neurons, and as an indicator of ΔΨm in intact tissues and isolated mitochondria. The high affinity of JC-1 staining reagents for mitochondria and its application in flow cytometry analysis makes it an indispensable tool for studying mitochondrial health and apoptosis.

Statistical analysis

Statistical analysis was conducted using GraphPad Prism 9.0. The normality of the data was assessed using the Kolmogorov-Smirnov test. Subsequently, Tukey's *post hoc* test was used for multiple group comparisons conducted through a one-way analysis of variance. Quantitative data are presented as mean ± SD. *P* value of < 0.05 were considered statistically significant.

RESULTS

GSE63992 of DEGs

The heatmap of gene differences and volcano plots are presented in the figures. In total, 34687 genes were identified based on the following criteria: |LogFC| > 2 and *P* value < 0.05 (3 genes); |LogFC| > 1 and *P* value < 0.05 (75 genes); and |LogFC| > 0.58 and *P* value < 0.05 (514 genes). Among identified genes, *FAM83D*, *FCN3*, *PLAC9*, *MMP23B*, *FAM107A*, *SELM*, *ISG15*, *AAAS*, *RASL10A*, and *KLC2* were upregulated in samples from diabetic individuals (Figure 1).

GSE63992 was performed on the Gene Set Enrichment Analysis result

The enriched genes demonstrated significant involvement in diverse biological processes, including the KEGG metabolism of xenobiotics by cytochrome P450, reactome biological oxidations, KEGG drug metabolism cytochrome P450, NABA ECM glycoproteins, KEGG retinol metabolism, NABA core matrisome, reactome drug ADME, KEGG steroid hormone biosynthesis, reactome phase II conjugation of compounds, and WP metapathway biotransformation phase I and II (Figure 2).

Functional and pathway enrichment

Figure 3A displays the expression of multiple inflammatory factors in the control and experimental groups. These factors

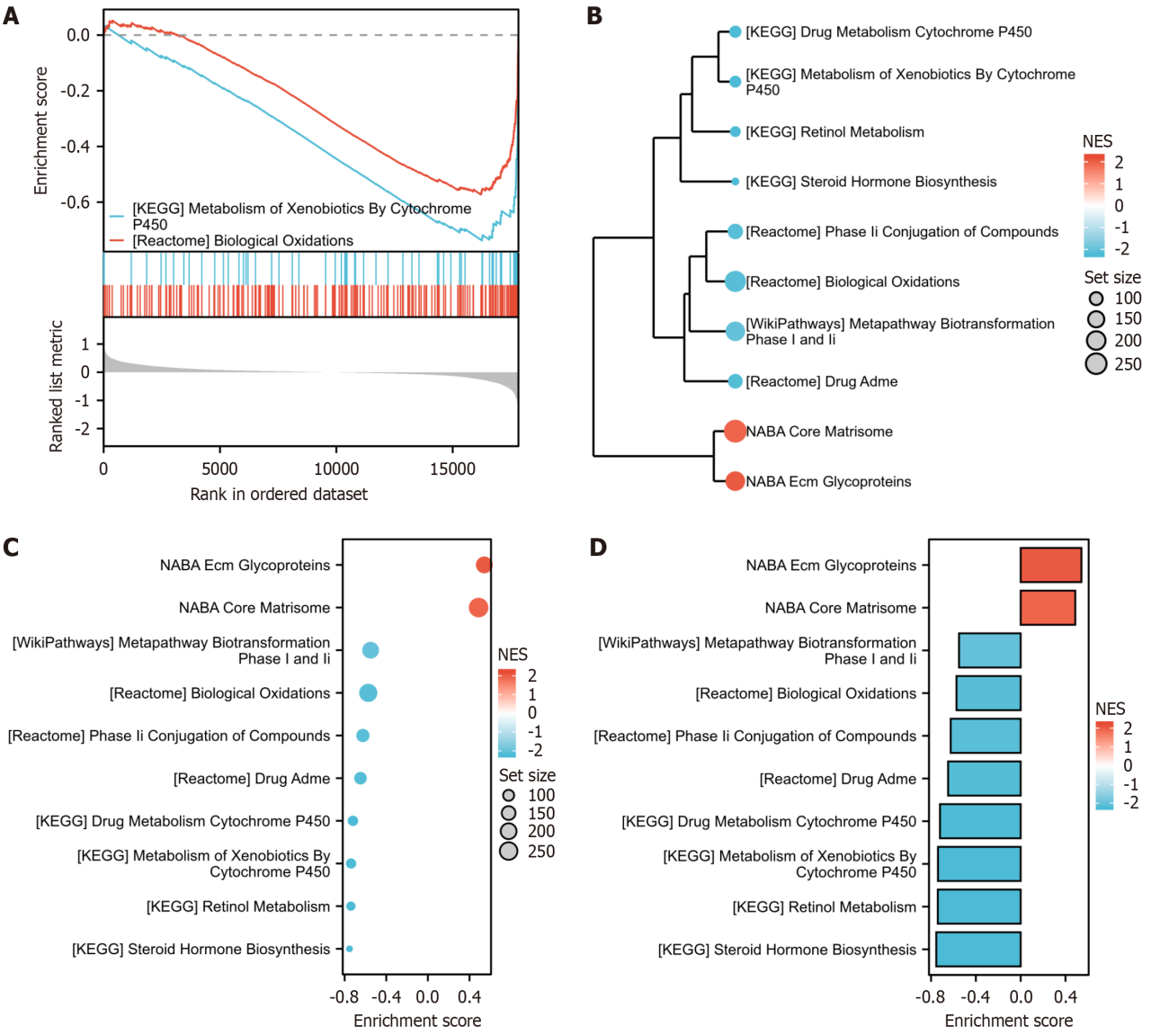

Figure 2 Functional and pathway enrichment analyses performed on the Gene Set Enrichment Analysis results. Functional and pathway enrichment analyses were conducted using DAVID to gain a comprehensive understanding of the role of the 10 differentially regulated pathways identified in the intestinal tissue dataset. A-D: Genes displaying significant enrichment in various biological processes: Reactome metabolism of fat-soluble vitamins, Kyoto Encyclopedia of Genes and Genomes complement and coagulation cascades, wp network map of the sarscov2 signaling pathway, reactome olfactory signaling pathway, reactome metabolism of vitamins and cofactors, reactome biological oxidations, reactome neutrophil degranulation, reactome metabolism of amino acids and derivatives, reactome metabolism of lipids, and reactome platelet activation signaling and aggregation. KEGG: Kyoto Encyclopedia of Genes and Genomes.

are primarily linked to cellular hormone metabolic processes, hormone metabolism, digestion, responses to toxic substances, retinol metabolism, collagen-containing extracellular matrix, brush border, and cluster of actin-based cell projections space. They are also enriched in various KEGG pathways (Figure 3).

Protein–protein interaction network analysis and inflammatory factor detection

The integrated analysis of LogFC and KEGG pathways highlighted the consistent involvement of MMP23B in these biological processes. Subsequently, a protein-protein interaction network comprising 11 DEGs was established using the STRING database and illustrated through the utilization of the Cytoscape tool (Figure 4A and B). In the diabetic nephropathy (DN) group, *MMP23B*, *MMP19*, and *HPX* were upregulated. Interestingly, DEX treatment reduced the expression levels of inflammatory markers in contrast to the DB group (Figure 4C-E).

The extent of STZ-induced intestinal injury is positively correlated with MMP23B in mice

We used MMP23B KO mice to understand the role of MMP23B in intestinal injury. Hematoxylin and eosin staining indicated less severe injury in MMP23B KO mice than in WT ones (Figure 5A-C). Immunofluorescence analysis indicated that the intestinal injury marker was markedly reduced after 24 hours of treatment (Figure 5D-I). Furthermore, protein expression levels of occludin and ZO-1 were markedly increased in the MMP23B KO group compared with the WT group, as observed by immunofluorescence (Figure 5J and K).

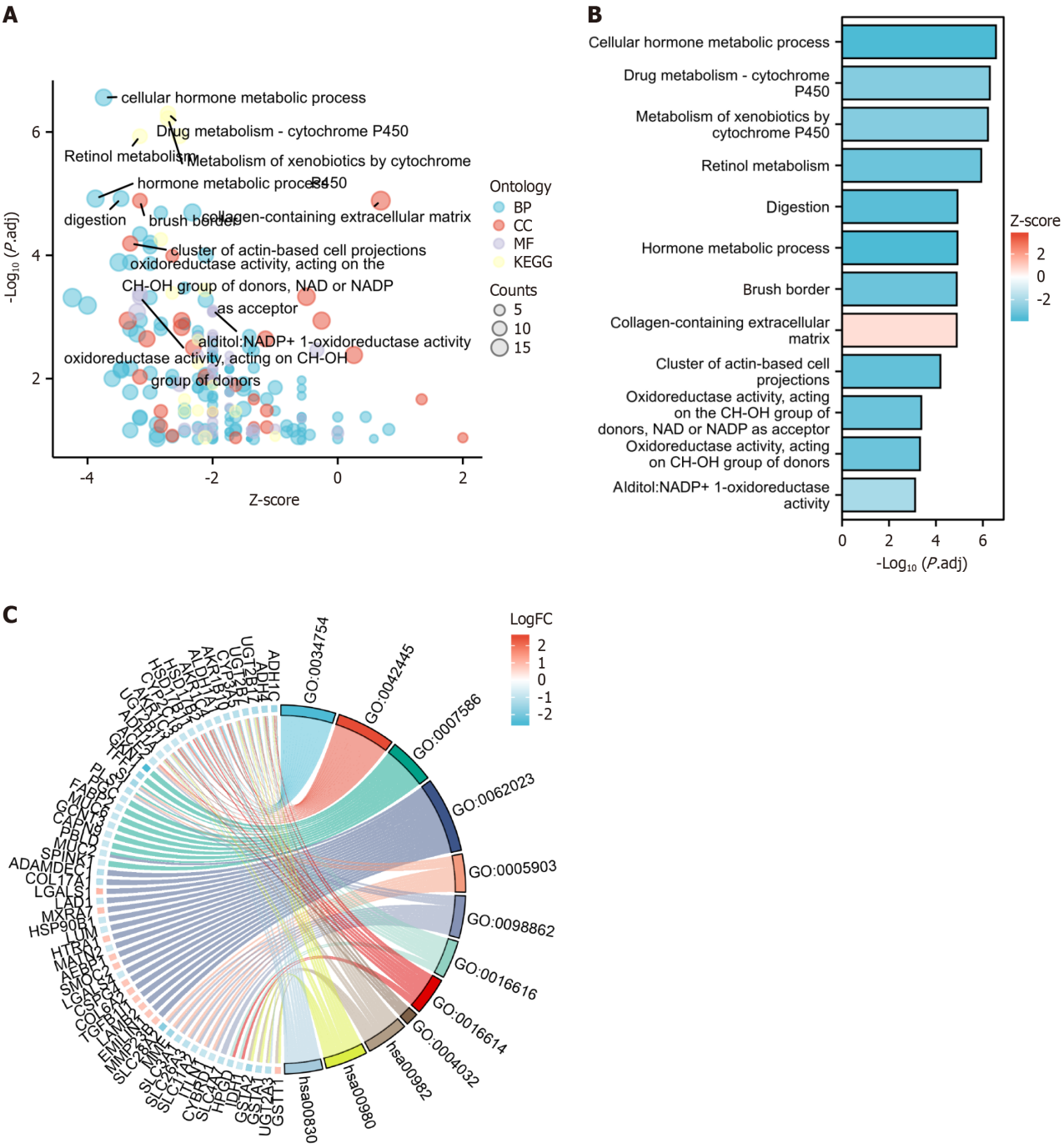

Figure 3 Functional and pathway enrichment. Functional and pathway enrichment analyses were conducted using DAVID to gain a comprehensive understanding of the role played by the 31 differentially expressed genes identified in the brain tissue dataset. A-C: Main identified pathways: Cellular hormone metabolic process, hormone metabolic process, digestion, response to toxic substance, retinol metabolic process, collagen-containing extracellular matrix, brush border, and cluster of actin-based cell projections. KEGG: Kyoto Encyclopedia of Genes and Genomes; BP: Biological process; CC: Cell composition; MF: Molecular function; GO:0034754: Cellular hormone metabolic process; GO:0042445: Hormone metabolic process; GO:0007586: Digestion; GO:0062023: Collagen-containing extracellular matrix; GO:0005903: Brush border; GO:0098862: Cluster of actin-based cell projections; GO:0016616: Oxidoreductase activity, acting on the CH-OH group of donors, NAD or NADP as acceptor; GO:0016614: Oxidoreductase activity, acting on CH-OH group of donors; GO:0004032: Alditol:NADP+ 1-oxidoreductase activity; hsa00982: Drug metabolism-cytochrome P450; hsa00980: Metabolism of xenobiotics by cytochrome P450; hsa00830: Retinol metabolism.

In vivo experiments demonstrated that macrophage clearance can improve intestinal function and the epithelium

To elucidate the role of macrophages in intestinal injury, we depleted macrophages using Cls in mice. Hematoxylin and eosin staining revealed mild injury in mice treated with Cls (Figure 6A-D). Immunofluorescence analysis demonstrated a significant induction in ZO-1 and reduction in CD86 levels after 24 hours of Cl treatment (Figure 6E-L). In addition, immunofluorescence analysis revealed a significant increase in the protein expression of CD86 and ZO-1 in MMP23B KO mice (Figure 6M and N).

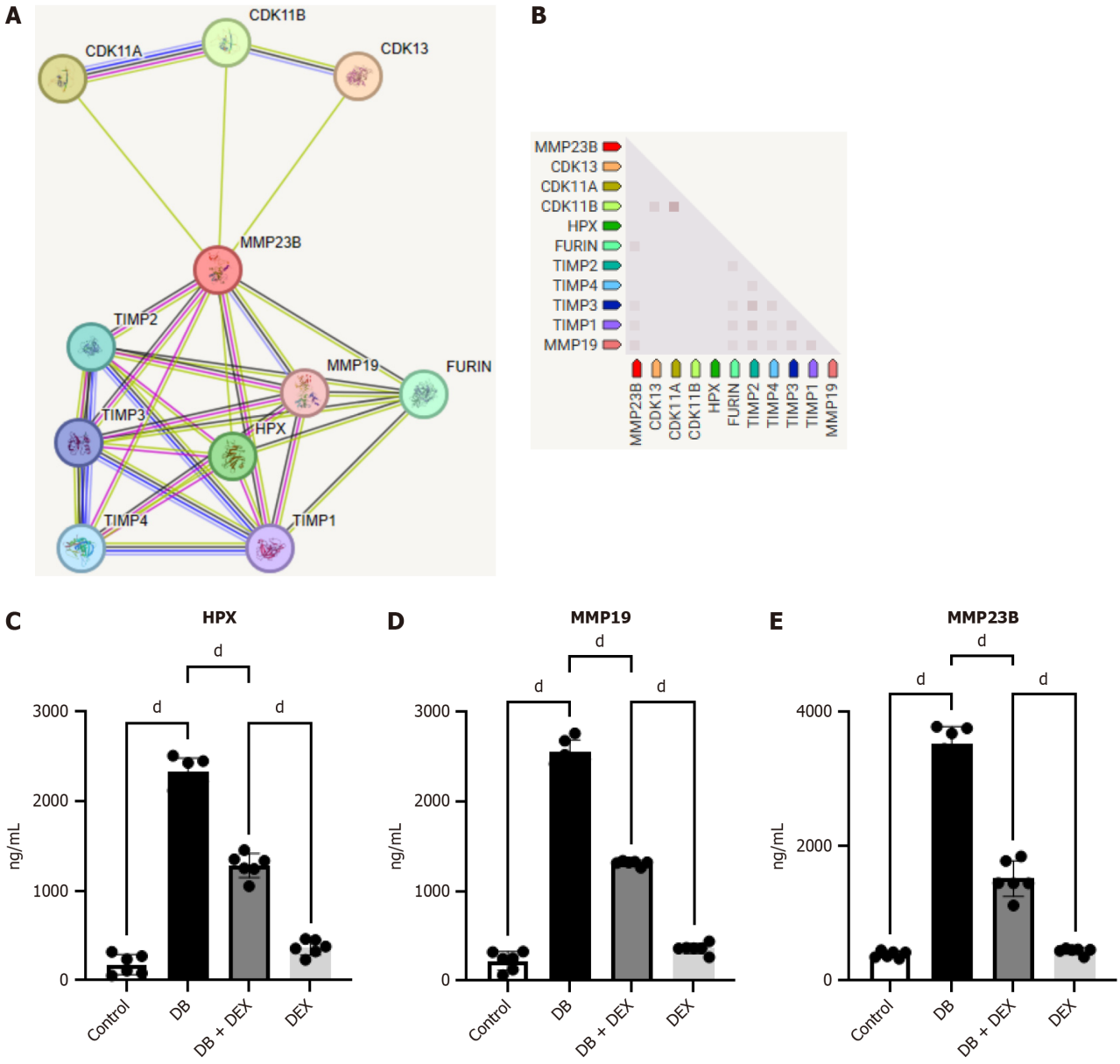

Figure 4 Protein-protein interaction network analysis and detected inflammatory factors. The protein-protein interaction network comprised five nodes representing molecular pathways and processes associated with the five core differentially expressed genes. A and B: Working modules were developed using the MCODE plugin for Cytoscape; C-E: The results revealed a module of nine genes. The expressions of *HPX*, *MMP19*, and *MMP23* were elevated in the diabetes group. The expression levels of inflammatory factors decreased upon dexmedetomidine compared with those in the control group. $^{d}P < 0.0001$. DB: Diabetes group; DEX: Dexmedetomidine.

Macrophage clearance can improve intestinal function and the epithelium in diabetic mice

Immunofluorescence analysis demonstrated significantly induced ZO-1 and occludin levels after 24 hours of Cl treatment (Figure 7A-J). Immunofluorescence analysis also revealed a significant decrease in the protein expression of occludin and ZO-1 in MMP23B KO mice (Figure 7K and L).

In vivo studies indicated that MMP23B KO induces the expression of arginase-1 and interleukin-10

In vivo experiments demonstrated that MMP23B KO resulted in M2 polarization. Following DB induction with STZ, the fluorescence intensity of arginase-1 (Arg-1) (Figure 8A-I) and interleukin (IL)-10 (Figure 8J-R) significantly decreased. Compared with the DB pretreatment levels, the fluorescence intensity levels were induced in MMP23B KO mice (Figure 8S and T).

In vitro models demonstrated that GM6001 inhibits intestinal epithelium injury

Fluorescence intensity levels of occludin (Figure 9A-C) and ZO-1 (Figure 9D-F) significantly decreased after MMP23B treatment compared with the baseline levels. Treating the MMP23B group with GM6001 improved the fluorescence intensity levels of occludin (Figure 9G) and ZO-1 (Figure 9H).

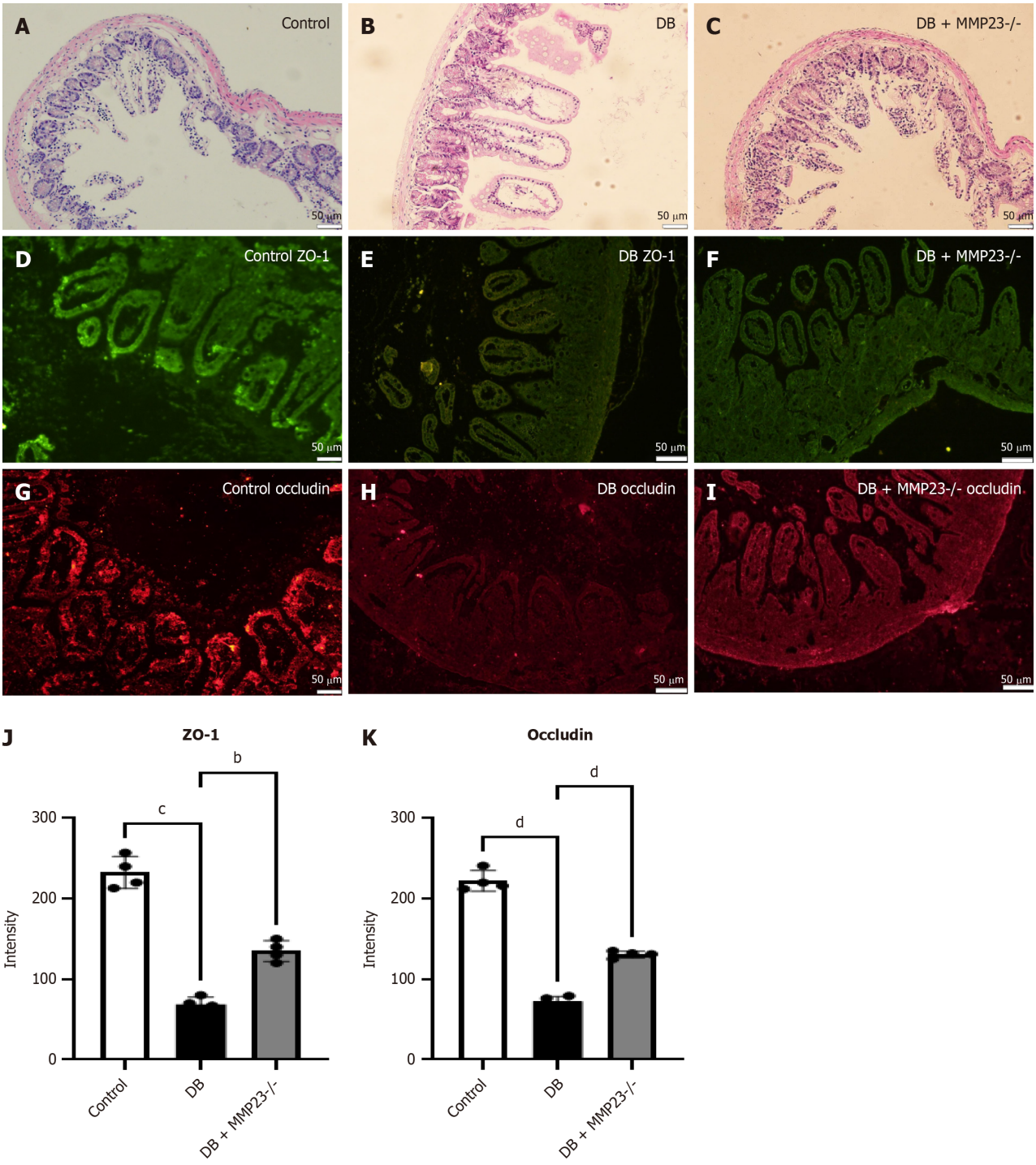

Figure 5 The severity of diabetes-induced intestinal injury was positively correlated with *MMP23* expression in mice. MMP23 KO mice were used to investigate the role of MMP23 in intestinal injury. A-C: Hematoxylin and eosin staining revealed a less severe injury in the intestines of MMP23 knockout mice; D-I: Immunofluorescence analysis demonstrated a significant reduction in the intestinal injury marker after 24 hours of treatment; J and K: The protein expression of occludin and ZO-1 was significantly upregulated following MMP23 knockout, as revealed by immunofluorescence analysis. Scale bar = 50 μm. $^{b}P < 0.01$, $^{c}P < 0.001$, $^{d}P < 0.0001$. DB: Diabetes group.

DEX induces mitochondrial impairment in Caco-2 cells in vitro

We investigated the effects of DEX on MMP23B-induced mitochondrial dysfunction in Caco-2 cells. Our results revealed that compared with a high glucose environment alone, treating cells with DEX decreases JC-1 monomer levels and increases ΔΨm, indicating that DEX can reverse the mitochondrial damage induced by high glucose (Figure 10).

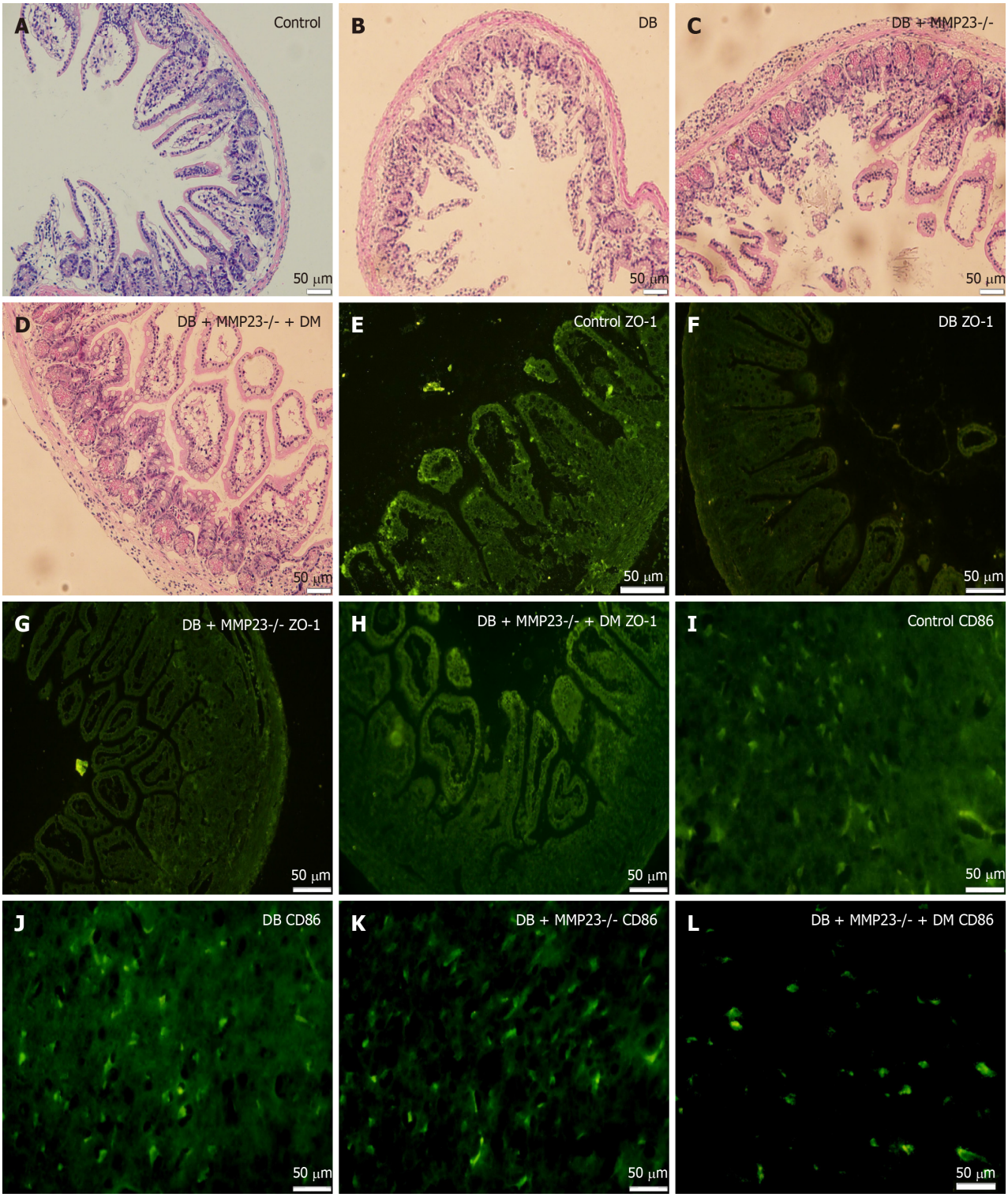
A
Control
50 μm
B
DB
50 μm
C
DB + MMP23-/-
50 μm
D
DB + MMP23-/- + DM
50 μm
E
Control ZO-1
50 μm
F
DB ZO-1
50 μm
G
DB + MMP23-/- ZO-1
50 μm
H
DB + MMP23-/- + DM ZO-1
50 μm
I
Control CD86
50 μm
J
DB CD86
50 μm
K
DB + MMP23-/- CD86
50 μm
L
DB + MMP23-/- + DM CD86
50 μm

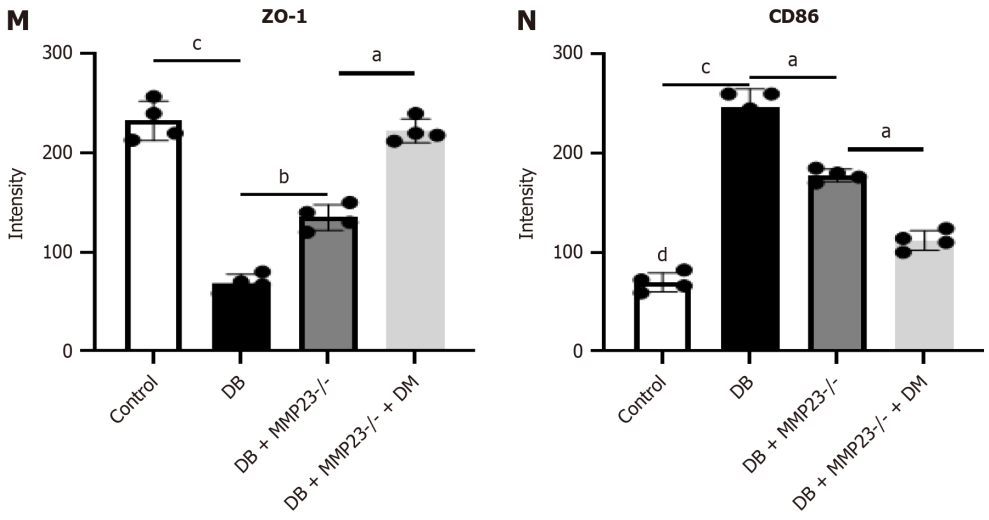

Figure 6 *In vivo* experiments demonstrated that macrophage clearance can improve intestinal function and epithelium integrity. We depleted macrophages using clodronate liposomes in mice to elucidate the role of macrophages in intestinal injury. A-D: Hematoxylin and eosin staining revealed less severe injury in mice treated with clodronate liposomes; E-L: Immunofluorescence analysis demonstrated a significant induction in ZO-1 and reduction in CD86 levels 24 hours after clodronate liposome treatment; M and N: Immunofluorescence analysis revealed a significant increase in the protein expression of CD86 and ZO-1 in MMP23 knockout mice. Scale bar = 50 μm. $^{a}P < 0.05$, $^{b}P < 0.01$, $^{c}P < 0.001$, $^{d}P < 0.0001$. DB: Diabetes group.

DISCUSSION

Our study reveals a novel role of DEX in modulating intestinal function, particularly in the context of diabetes. DEX significantly influences intestinal motility and immune responses by interacting with the MMP23B pathway[19,20]. This finding is pivotal as it suggests that DEX counteracts diabetes-related intestinal tissue damage by regulating the activity of M1 macrophages and expression of MMP23B, a key inflammatory factor.

In the diabetic state, the intestinal microenvironment is altered, leading to inflammation and subsequent damage. This state is characterized by the release of cytokines, which can cause tissue damage when dysregulated[21,22]. Our bioinformatics analysis revealed that in addition to MMP19 and MMP8, MMP23B was upregulated in the diabetic group, indicating its potential role in the pathogenesis of diabetes-related intestinal complications.

Furthermore, our mechanistic experiments revealed that DEX decreased the expression levels of these inflammatory factors, suggesting its protective effect on intestinal tissues. MMP23B, with its capacity to degrade extracellular matrix proteins, is implicated in various biological processes, including central nervous system development and inflammatory responses. Its modulation by DEX may be central to mitigating diabetes-induced intestinal disruptions. Elucidating the effect of DEX on MMP23B can provide a new perspective on the management of diabetes-related gastrointestinal complications and open avenues for future research into targeted therapies that leverage this pathway for intestinal protection and repair.

These cytokines are crucial in regulating immune responses and the inflammatory process, but their excessive or improper release may damage intestinal tissues. Through bioinformatics analysis, we identified three genes with Log|FC| > 2 and *P* value < 0.05 in the DB group, among which the expression of the inflammatory factor MMP23B was elevated. Further gene enrichment analysis revealed cellular metabolism and extracellular matrix glycoprotein secretion. In the DN group, the expression of *MMP23B*, *MMP19*, and *MMP8* was elevated. DEX decreased the expression levels of inflammatory factors compared with those in the DB group.

MMP23B is involved in central nervous system development, inflammatory responses, and invasion and metastasis. It has a typical metalloproteinase structure, including a signal peptide sequence, a protease active site domain, and a cysteine/cysteine repeat sequence. The zinc ions in the MMP23B active domain can participate in the degradation of extracellular matrix proteins, playing a role in reshaping the extracellular matrix and regulating cellular behavior[23,24]. However, the impact of MMP23B on intestinal macrophages remains unclear.

M1 macrophages, also known as classically activated macrophages, promote inflammation and host defense in response to infection or injury[25,26]. In diabetes-related intestinal tissue, M1 macrophages can contribute to the immune response and tissue damage. During diabetes, the intestinal tissue can be exposed to bacterial pathogens or their components due to increased intestinal permeability. This exposure triggers an inflammatory response, leading to M1 macrophage activation in the intestinal tissue. These cytokines contribute to recruiting and activating other immune cells, enhancing the inflammatory response in diabetes-related intestinal tissues[27,28]. M1 macrophages have enhanced phagocytic capacity and microbial killing abilities. They can engulf and eliminate pathogens, thereby helping in controlling infection in individuals with diabetes. However, excessive M1 macrophage activation can lead to tissue damage due to the release of cytotoxic molecules. Suppression of IL-10 promotes inflammatory reactions and impairs M1 macrophage polarization by targeting MMP23B, which is critical in macrophage polarization[29-31].

Our study demonstrated that MMP23B is responsible for macrophage polarization, highlighting its unique role in M1 macrophage polarization and potential contribution to the development of diabetes-related intestinal damage in mice.

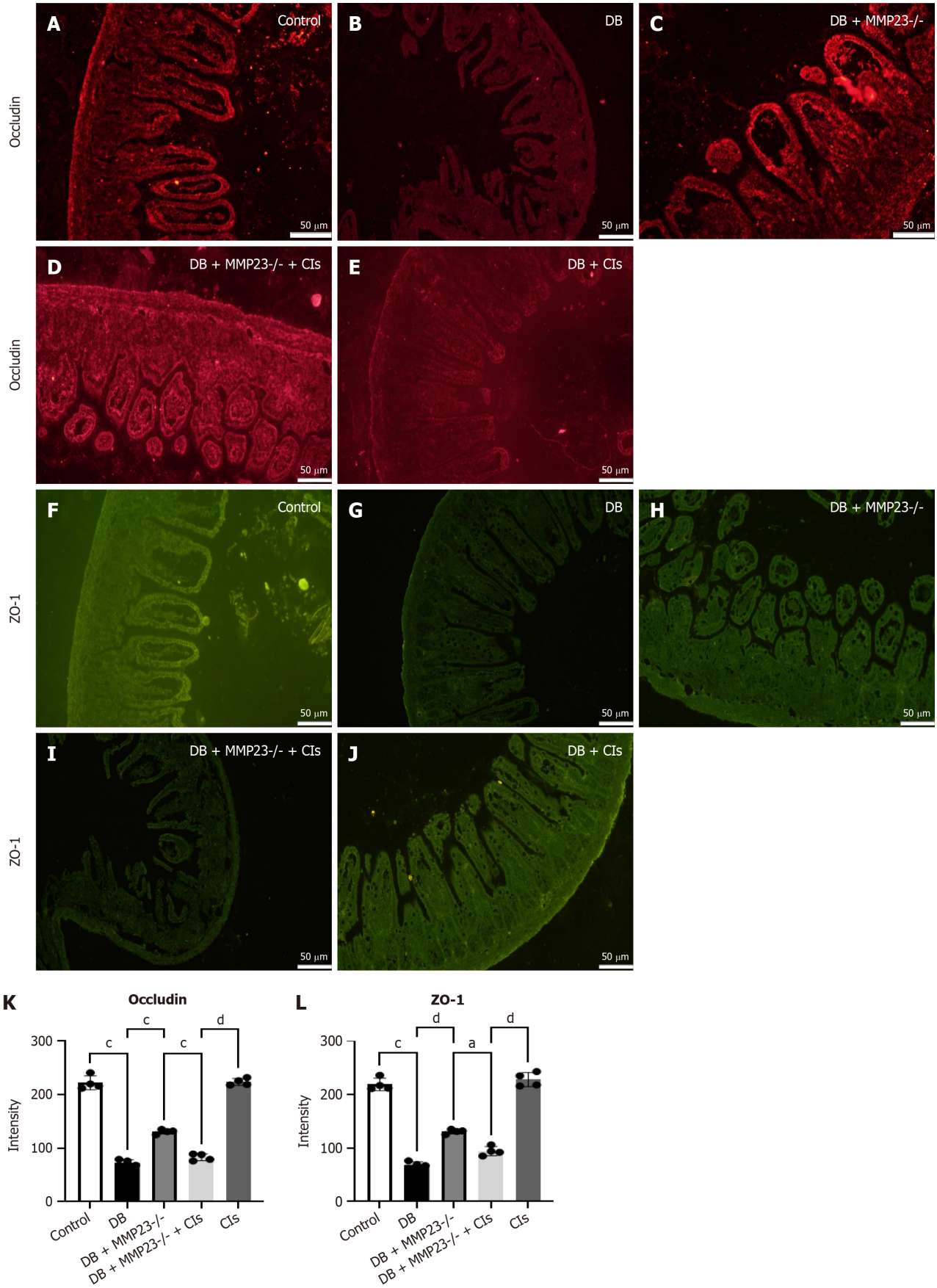

Figure 7 Macrophage clearance enhances intestinal function and improves the epithelium in diabetes mice. A-J: After 24 hours of treatment with clodronate liposomes, immunofluorescence analysis revealed a substantial decrease in ZO-1 and occludin levels; K and L: The immunofluorescence analysis demonstrated a notable elevation in the protein expression of occludin and ZO-1 following DB. Scale bar = 50 μm. $^{a}P < 0.05$, $^{c}P < 0.001$, $^{d}P < 0.0001$. DB: Diabetes group; CIs: Clodronate liposomes.

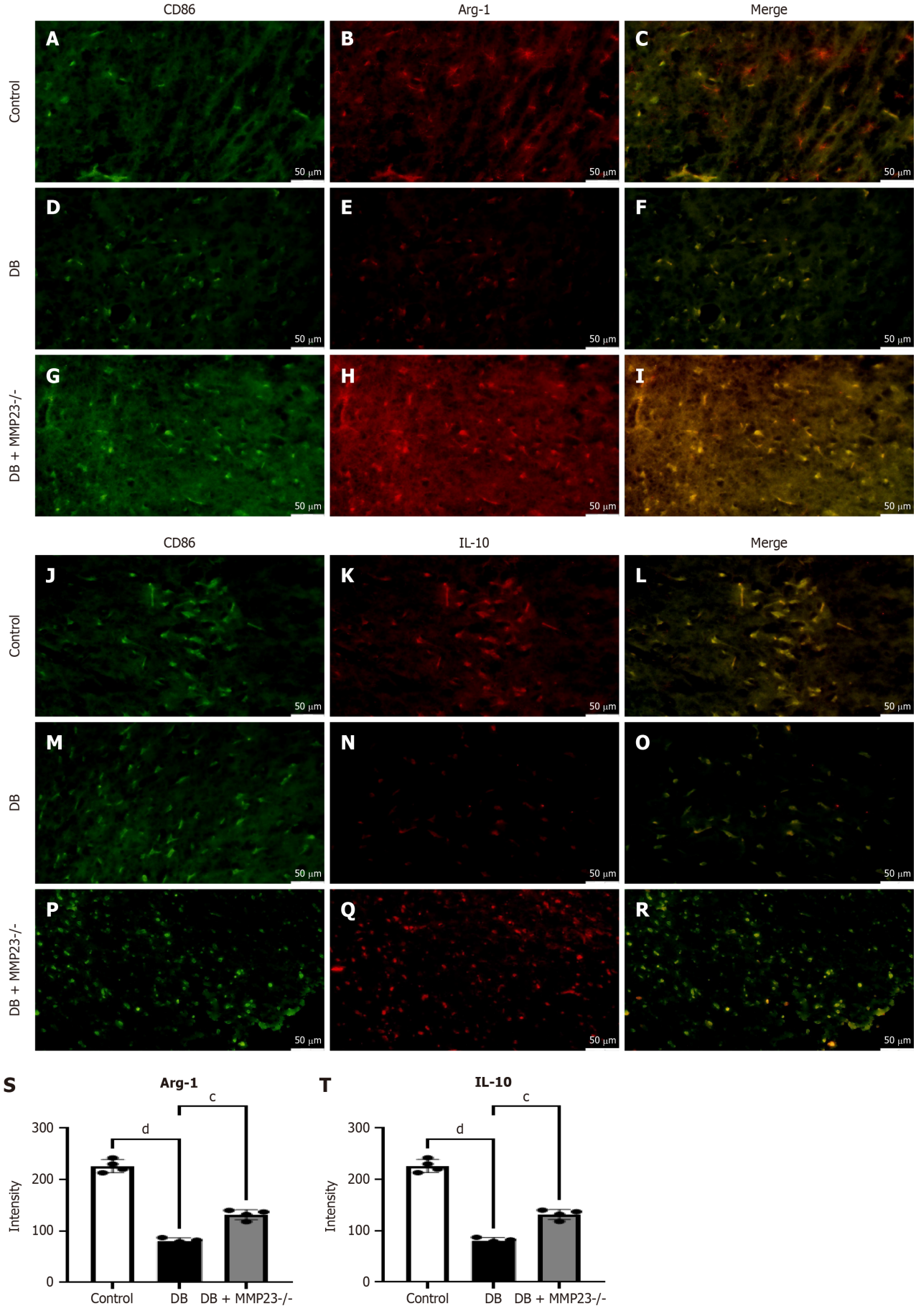

Figure 8 *In vivo* studies demonstrated that MMP23 knockout upregulates arginase-1 and interleukin-10. A-R: MMP23 knockout led to M2

polarization. After inducing diabetes with the diabetes treatment, the fluorescence intensity of arginase-1 (A-I) and interleukin-10 (J-R) significantly decreased compared with that before treatment; S and T: Indicating fluorescence intensity levels after MMP23 knockout treatment. Scale bar = 50 μm. $^{c}P < 0.001$, $^{d}P < 0.0001$. DB: Diabetes group; Arg-1: Arginase-1; IL-10: Interleukin-10.

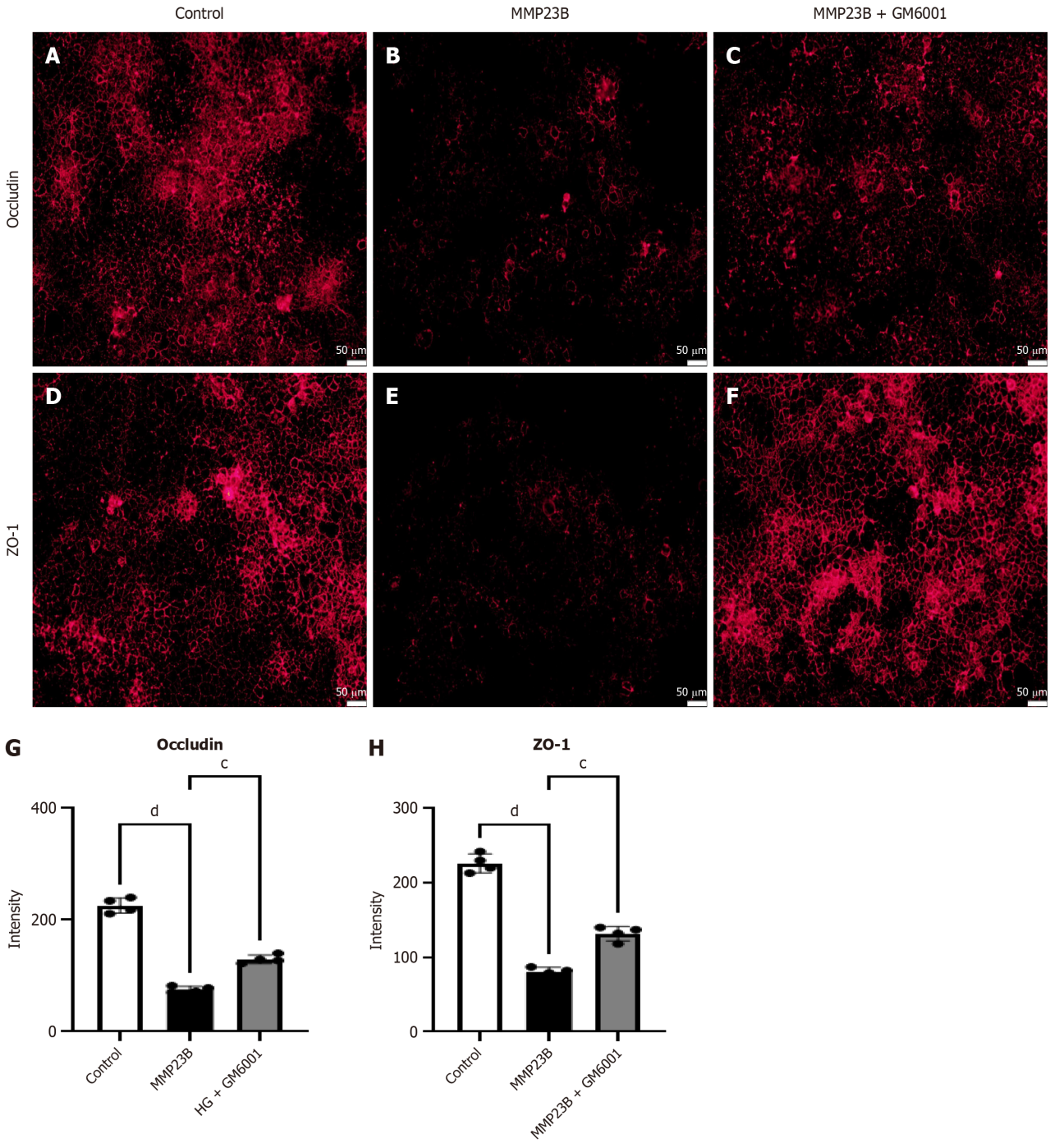

Figure 9 *In vitro* models demonstrated that GM6001 inhibits intestinal epithelium damage. A-F: Following lipopolysaccharide treatment, a substantial decrease was observed in the fluorescence intensity levels of occludin (A-C) and ZO-1 (D-F) compared with the baseline levels; G and H: Administering GM6001 to the MMP23B group improved the fluorescence intensity levels of occludin (G) and ZO-1 (H). Scale bar = 50 μm. $^{c}P < 0.001$, $^{d}P < 0.0001$. HG: High glucose.

Hematoxylin and eosin staining indicated less severe injury in MMP23B KO mice. Immunofluorescence analysis indicated that the intestinal injury marker was markedly reduced after 24 hours of treatment. Furthermore, the protein expression of occludin and ZO-1 was markedly increased after MMP23B KO, as observed *via* immunofluorescence analysis.

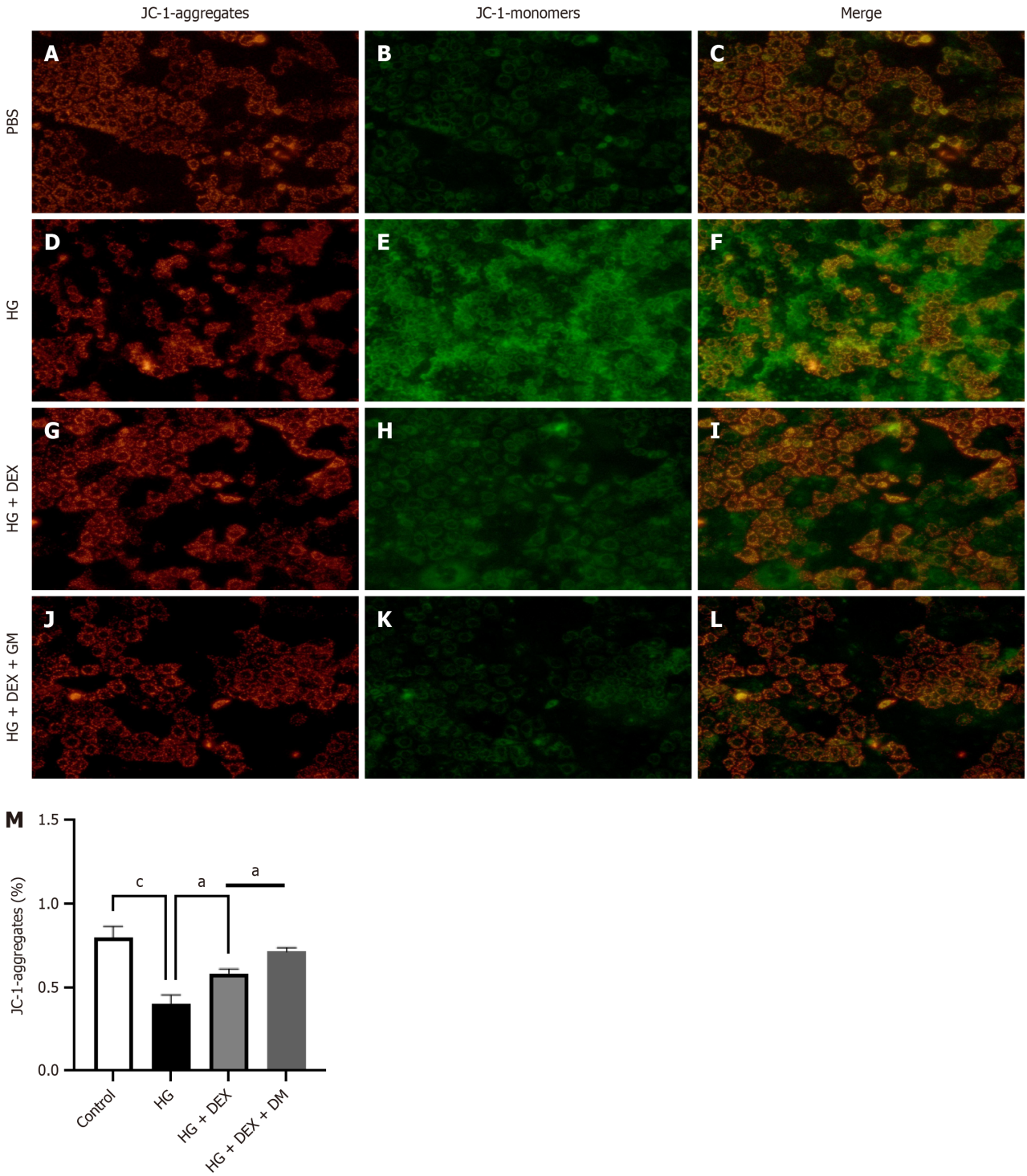

Figure 10 Dexmedetomidine induces mitochondrial impairment in Caco-2 cells *in vitro*. A-M: During inflammation, mitochondrial oxidative energy metabolism plays a pivotal role in maintaining the integrity of the gut epithelial barrier. We investigated the potential effects of dexmedetomidine on high glucose-induced mitochondrial dysfunction in Caco-2 cells. Comparative analysis revealed that dexmedetomidine treatment, as opposed to high glucose treatment alone, substantially reduced mitochondrial dysfunction, manifested through reduced levels of JC-1 monomers and enhanced ΔΨm. $^{a}P < 0.05$, $^{c}P < 0.001$. HG: High glucose; DEX: Dexmedetomidine; PBS: Phosphate buffer saline; GM: GM6001.

While the role of MMP23B in the intestine remains unclear, our study revealed that knocking out MMP23B downregulates the intestinal tight junction (TJ) proteins ZO-1 and occludin and upregulates proinflammatory factors. These results provide a deeper understanding of *MMP23B*. Previous studies have reported that IL-1β stimulates periodontal inflammation during RR, inducing IL-10 and tumor necrosis factor-α synthesis and secretion. However, the initial source of IL-10 and the M2 subtype that possesses anti-inflammatory properties remain unclear. ZO-1, the earliest discovered epithelial TJ protein, is crucial in cell function and permeability[32-36]. Accordingly, blocking or removing ZO-1 in cells did not prevent the assembly of TJs or hinder the development of barrier functions.

We depleted macrophages using Cls in mice to elucidate the role of macrophages in intestinal injury[37,38]. Hematoxylin and eosin staining revealed mild injury in mice treated with Cls. Immunofluorescence analysis demonstrated a significant reduction in ZO-1 and CD86 levels after 24 hours of Cl treatment and a significant increase in the protein expression of CD86 and ZO-1 after MMP23 knockout. *In vivo* experiments revealed that knocking out MMP23B led to M2 polarization.

Upon STZ induction through DB treatment, fluorescence intensity levels of Arg-1 and IL-10 were notably reduced. Compared with the pretreatment levels, the fluorescence intensity levels displayed a decrease after MMP23B KO. Mitochondria have various critical functions in cells and are closely related to cell damage. During energy production, mitochondria produce some byproducts, such as reactive oxygen species. When reactive oxygen species are produced excessively, they may lead to oxidative stress, thereby damaging mitochondria and other organelles and further exacerbating cell damage[39]. The findings of the present study indicated that treatment with DEX, as opposed to treatment with MMP23B alone, significantly reduced mitochondrial dysfunction, as evidenced by decreased levels of JC-1 monomers and an improved $\Delta\Psi m$.

Although animal models have provided valuable insights, the complexity of the human diabetic intestinal damage has not been fully understood. Careful consideration and rigorous validation are required to translate our findings from mouse experiments into clinical applications. Moreover, further investigation into the exact role of MMP23B in diabetes-related inflammation is needed.

CONCLUSION

In conclusion, our study indicated that DEX reduces MMP23B, which is a potential contributor to intestinal barrier dysfunction that may induce diabetes, affecting TJ changes through mitochondrial dysfunction.

FOOTNOTES

Author contributions: Luo FQ designed the research study; Lu M, Guo XW, Zhang FF, and Wu DH performed the research; Xie D contributed new reagents and analytic tools; Lu M, Guo XW, Zhang FF, Wu DH, and Luo FQ analyzed the data and wrote the manuscript. All authors have read and approved the final manuscript.

Institutional animal care and use committee statement: This study was reviewed and approved by the Medical Ethics Committee of Xinhua Hospital, Shanghai Jiao Tong University School of Medicine (Approval No. XHEC-STCSM-2021-028).

Conflict-of-interest statement: All the authors report no relevant conflicts of interest for this article.

Data sharing statement: Raw data can be obtained by contacting the corresponding author.

ARRIVE guidelines statement: The authors have read the ARRIVE guidelines, and the manuscript was prepared and revised according to the ARRIVE guidelines.

Country of origin: China

ORCID number: Man Lu 0009-0005-5964-1536; Dan-Hong Wu 0000-0002-2521-932X; Feng-Qin Luo 0009-0009-1255-2228.

S-Editor: Wang JJ
L-Editor: A
P-Editor: Zheng XM

REFERENCES

1 **Elashi AA**, Toor SM, Umlai UI, Al-Sarraj YA, Taheri S, Suhre K, Abou-Samra AB, Albagha OME. Correction: Genome-wide association study and trans-ethnic meta-analysis identify novel susceptibility loci for type 2 diabetes mellitus. *BMC Med Genomics* 2024; **17**: 131 [PMID: 38755684 DOI: 10.1186/s12920-024-01903-w]

2 **Merlo EM**, Tutino R, Myles LAM, Lia MC, Minasi D. Alexithymia, intolerance to uncertainty and mental health difficulties in adolescents with Type 1 diabetes mellitus. *Ital J Pediatr* 2024; **50**: 99 [PMID: 38755698 DOI: 10.1186/s13052-024-01647-4]

3 **Zeng X**, Huang S, Ye X, Song S, He J, Hu L, Deng S, Liu F. Impact of HbA1c control and type 2 diabetes mellitus exposure on the oral microbiome profile in the elderly population. *J Oral Microbiol* 2024; **16**: 2345942 [PMID: 38756148 DOI: 10.1080/20002297.2024.2345942]

4 **Ahn JH**, Lopez L, Tibbs T, Yu YR, Tighe R, Denson L, Arthur J. Zinc restriction by intestinal *E. coli* - produced Yersiniabactin activates HIF-

1α in macrophages to promote CD-associated fibrosis. *Inflamm Bowel Dis* 2024; **30**: S62-S62 [DOI: 10.1093/ibd/izae020.131]

5 **Zhang S**, Zhang C, Yan H, Yang L, Shi N, Liu C, Chen Y. Sacral Nerve Stimulation Alleviates Intestinal Inflammation Through Regulating the Autophagy of Macrophages and Activating the Inflammasome Mediated by a Cholinergic Antiinflammatory Pathway in Colitis Rats. *Neuromodulation* 2024; **27**: 302-311 [PMID: 36740464 DOI: 10.1016/j.neurom.2023.01.005]

6 **Zhu L**, Dou Z, Wu W, Hou Q, Wang S, Yuan Z, Li B, Liu J. Ghrelin/GHSR Axis Induced M2 Macrophage and Alleviated Intestinal Barrier Dysfunction in a Sepsis Rat Model by Inactivating E2F1/NF-κB Signaling. *Can J Gastroenterol Hepatol* 2023; **2023**: 1629777 [PMID: 38187112 DOI: 10.1155/2023/1629777]

7 **Deng S**, Li W, Li Z, Wang P, Ma Q. Bright luminescent Zn(2)GeO(4):Mn NP/MXene hydrogel-based ECL biosensor for glioblastoma diagnosis. *Talanta* 2024; **276**: 126214 [PMID: 38718647 DOI: 10.1016/j.talanta.2024.126214]

8 **Liu C**, Xu R. Dexmedetomidine protects H9C2 rat cardiomyocytes against hypoxia/reoxygenation injury by regulating the long non-coding RNA colon cancer-associated transcript 1/microRNA-8063/Wnt/β-catenin axis. *Bioengineered* 2022; **13**: 13300-13311 [PMID: 35635079 DOI: 10.1080/21655979.2022.2080420]

9 **Pluskiewicz W**, Werner A, Bach M, Adamczyk P, Drozdzowska B. Fracture risk prediction in postmenopausal women from GO Study: the comparison between FRAX, Garvan, and POL-RISK algorithms. *Arch Osteoporos* 2024; **19**: 39 [PMID: 38755326 DOI: 10.1007/s11657-024-01392-5]

10 **Rocca MA**, Valsasina P, Romanò F, Tedone N, Amato MP, Brichetto G, Boccia VD, Chataway J, Chiaravalloti ND, Cutter G, Dalgas U, DeLuca J, Farrell RA, Feys P, Freeman J, Inglese M, Meza C, Motl RW, Salter A, Sandroff BM, Feinstein A, Filippi M; Cogex Research Team. Cognitive rehabilitation effects on grey matter volume and Go-NoGo activity in progressive multiple sclerosis: results from the CogEx trial. *J Neurol Neurosurg Psychiatry* 2024 [PMID: 38754979 DOI: 10.1136/jnnp-2024-333460]

11 **Chen S**, Li Y, Song W, Cheng Y, Gao Y, Xie L, Huang M, Yan X. Insulin eye drops improve corneal wound healing in STZ-induced diabetic mice by regulating corneal inflammation and neuropeptide release. *BMC Ophthalmol* 2024; **24**: 155 [PMID: 38594682 DOI: 10.1186/s12886-024-03436-3]

12 **Tabaa MME**, Tabaa MME, Rashad E, Elballal MS, Elazazy O. Harmine alleviated STZ-induced rat diabetic nephropathy: A potential role *via* regulating AMPK/Nrf2 pathway and deactivating ataxia-telangiectasia mutated (ATM) signaling. *Int Immunopharmacol* 2024; **132**: 111954 [PMID: 38554444 DOI: 10.1016/j.intimp.2024.111954]

13 **Culemann S**, Knab K, Euler M, Wegner A, Garibagaoglu H, Ackermann J, Fischer K, Kienhöfer D, Crainiciuc G, Hahn J, Grüneboom A, Nimmerjahn F, Uderhardt S, Hidalgo A, Schett G, Hoffmann MH, Krönke G. Addendum: Stunning of neutrophils accounts for the anti-inflammatory effects of clodronate liposomes. *J Exp Med* 2023; **220** [PMID: 37294312 DOI: 10.1084/jem.2022052506022023a]

14 **Mochalova EN**, Egorova EA, Komarova KS, Shipunova VO, Khabibullina NF, Nikitin PI, Nikitin MP. Comparative Study of Nanoparticle Blood Circulation after Forced Clearance of Own Erythrocytes (Mononuclear Phagocyte System-Cytoblockade) or Administration of Cytotoxic Doxorubicin- or Clodronate-Loaded Liposomes. *Int J Mol Sci* 2023; **24** [PMID: 37445804 DOI: 10.3390/ijms241310623]

15 **Fang M**, Yin W, Qiu C, Song T, Lin B, Wang Y, Xiong H, Wu S. Stromal B Lymphocytes Affecting Prognosis in Triple-Negative Breast Cancer by Opal/TSA Multiplexed Immunofluorescence. *Int J Womens Health* 2024; **16**: 755-767 [PMID: 38706691 DOI: 10.2147/IJWH.S444202]

16 **Tomimatsu K**, Fujii T, Bise R, Hosoda K, Taniguchi Y, Ochiai H, Ohishi H, Ando K, Minami R, Tanaka K, Tachibana T, Mori S, Harada A, Maehara K, Nagasaki M, Uchida S, Kimura H, Narita M, Ohkawa Y. Precise immunofluorescence canceling for highly multiplexed imaging to capture specific cell states. *Nat Commun* 2024; **15**: 3657 [PMID: 38719795 DOI: 10.1038/s41467-024-47989-9]

17 **Roelofs L**, Frössling J, Rosander A, Bjerketorp J, Belaghi RA, Hansson I, Frosth S. Digital dermatitis in Swedish dairy herds assessed by ELISA targeting Treponema phagedenis in bulk tank milk. *BMC Vet Res* 2024; **20**: 168 [PMID: 38698418 DOI: 10.1186/s12917-024-04021-y]

18 **Małota K**, Student S, Świątek P. Low mitochondrial activity within developing earthworm male germ-line cysts revealed by JC-1. *Mitochondrion* 2019; **44**: 111-121 [PMID: 29398303 DOI: 10.1016/j.mito.2018.01.007]

19 **Ekkapat G**, Kampitak W, Theerasuwipakorn N, Kittipongpattana J, Engsusophon P, Phannajit J, Chokengarmwong N. A Comparison of Efficacy between Low-dose Dexmedetomidine and Propofol for Prophylaxis of Postoperative Delirium in Elderly Patients Undergoing Hip Fracture Surgery: A Randomized Controlled Trial. *Indian J Crit Care Med* 2024; **28**: 467-474 [PMID: 38738208 DOI: 10.5005/jp-journals-10071-24710]

20 **Sun Y**, Darmani NA. A Comparative Study of the Antiemetic Effects of α(2)-Adrenergic Receptor Agonists Clonidine and Dexmedetomidine against Diverse Emetogens in the Least Shrew (Cryptotis parva) Model of Emesis. *Int J Mol Sci* 2024; **25** [PMID: 38731821 DOI: 10.3390/ijms25094603]

21 **Frühbeck G**, Gómez-Ambrosi J, Ramírez B, Becerril S, Rodríguez A, Mentxaka A, Valentí V, Moncada R, Reina G, Baixauli J, Casado M, Silva C, Escalada J, Catalán V. Decreased expression of the NLRP6 inflammasome is associated with increased intestinal permeability and inflammation in obesity with type 2 diabetes. *Cell Mol Life Sci* 2024; **81**: 77 [PMID: 38315242 DOI: 10.1007/s00018-024-05124-3]

22 **Liu X**, Fang H, Pan L, Zhang P, Lin H, Gao H, Ye C, Mao D, Luo Y. S-amlodipine induces liver inflammation and dysfunction through the alteration of intestinal microbiome in a rat model. *Gut Microbes* 2024; **16**: 2316923 [PMID: 38400721 DOI: 10.1080/19490976.2024.2316923]

23 **Allione A**, Pardini B, Viberti C, Giribaldi G, Turini S, Di Gaetano C, Guarrera S, Cordero F, Oderda M, Allasia M, Gontero P, Sacerdote C, Vineis P, Matullo G. MMP23B expression and protein levels in blood and urine are associated with bladder cancer. *Carcinogenesis* 2018; **39**: 1254-1263 [PMID: 30052775 DOI: 10.1093/carcin/bgy098]

24 **Pardini B**, Allione A, Viberti C, Giribaldi G, Turini S, Gaetano CD, Guarrera S, Cordero F, Oderda M, Allasia M, Gontero P, Sacerdote C, Naccarati A, Vineis P, Matullo G. Abstract 1258: MMP23B expression and protein levels in blood and urine are associated with bladder cancer risk. *Cancer Res* 2018; **78**: 1258 [DOI: 10.1158/1538-7445.AM2018-1258]

25 **Choi JY**, Byeon HW, Park SO, Uyangaa E, Kim K, Eo SK. Inhibition of NADPH oxidase 2 enhances resistance to viral neuroinflammation by facilitating M1-polarization of macrophages at the extraneural tissues. *J Neuroinflammation* 2024; **21**: 115 [PMID: 38698374 DOI: 10.1186/s12974-024-03078-8]

26 **Li Y**, Guo X, Zhan P, Huang S, Chen J, Zhou Y, Jiang W, Chen L, Lin Z. TRPV1 Regulates Proinflammatory Properties of M1 Macrophages in Periodontitis Via NRF2. *Inflammation* 2024 [PMID: 38700791 DOI: 10.1007/s10753-024-02024-3]

27 **Gonciarz W**, Piątczak E, Chmiela M. The influence of Salvia cadmica Boiss. extracts on the M1/M2 polarization of macrophages primed with Helicobacter pylori lipopolysaccharide in conjunction with NF-kappa B activation, production of cytokines, phagocytic activity and total DNA methylation. *J Ethnopharmacol* 2023; **310**: 116386 [PMID: 36921911 DOI: 10.1016/j.jep.2023.116386]

28 **Mathiesen CBK**, Rudjord-Levann AM, Gad M, Larsen J, Sellebjerg F, Pedersen AE. Cladribine inhibits secretion of pro-inflammatory cytokines and phagocytosis in human monocyte-derived M1 macrophages in-vitro. *Int Immunopharmacol* 2021; **91**: 107270 [PMID: 33360830

DOI: 10.1016/j.intimp.2020.107270]

29 **Honjoh K**, Nakajima H, Hirai T, Watanabe S, Matsumine A. Relationship of Inflammatory Cytokines From M1-Type Microglia/Macrophages at the Injured Site and Lumbar Enlargement With Neuropathic Pain After Spinal Cord Injury in the CCL21 Knockout (plt) Mouse. *Front Cell Neurosci* 2019; **13**: 525 [PMID: 31824269 DOI: 10.3389/fncel.2019.00525]

30 **Inoue Y**, Kamiya T, Hara H. Increased expression of ELOVL7 contributes to production of inflammatory cytokines in THP-1 cell-derived M1-like macrophages. *J Clin Biochem Nutr* 2023; **72**: 215-224 [PMID: 37251958 DOI: 10.3164/jcbn.22-69]

31 **Jędrzejewski T**, Pawlikowska M, Sobocińska J, Wrotek S. Protein-Bound Polysaccharides from Coriolus Versicolor Fungus Disrupt the Crosstalk Between Breast Cancer Cells and Macrophages through Inhibition of Angiogenic Cytokines Production and Shifting Tumour-Associated Macrophages from the M2 to M1 Subtype. *Cell Physiol Biochem* 2020; **54**: 615-628 [PMID: 32559360 DOI: 10.33594/000000244]

32 **Georgiadis A**, Tschernutter M, Bainbridge JWB, Balaggan KS, Mowat F, West EL, Munro PMG, Thrasher AJ, Matter K, Balda MS, Ali RR. Correction: The Tight Junction Associated Signalling Proteins ZO-1 and ZONAB Regulate Retinal Pigment Epithelium Homeostasis in Mice. *PLoS One* 2023; **18**: e0295782 [PMID: 38060570 DOI: 10.1371/journal.pone.0295782]

33 **Schmidt A**, Finegan T, Häring M, Kong D, Fletcher AG, Alam Z, Grosshans J, Wolf F, Peifer M. Polychaetoid/ZO-1 strengthens cell junctions under tension while localizing differently than core adherens junction proteins. *Mol Biol Cell* 2023; **34**: ar81 [PMID: 37163320 DOI: 10.1091/mbc.E23-03-0077]

34 **Wang K**, Hongyan Q, Lassegue B, Eaton DCC, Song C, Mu J, Griendling KK, Hernandes MS. Abstract 12294: Poldip2 Mediates Brain Vascular Permeability by Regulating ZO-1 Phosphorylation and Localization at the Interendothelial Border. *Circulation* 2023; **148** [DOI: 10.1161/circ.148.suppl_1.12294]

35 **Wu H**, Wu L, Yu W, Gu C, Li Y, Chen K, Zhang L, Qian F. Veronica linariifolia subsp. dilatata ameliorates LPS-induced acute lung injury by attenuating endothelial cell barrier dysfunction *via* EGFR/Akt/ZO-1 pathway. *J Ethnopharmacol* 2024; **321**: 117545 [PMID: 38056533 DOI: 10.1016/j.jep.2023.117545]

36 **Zhuang X**, Martin TA, Ruge F, Zeng JJ, Li XA, Khan E, Dou Q, Davies E, Jiang WG. Expression of Claudin-9 (CLDN9) in Breast Cancer, the Clinical Significance in Connection with Its Subcoat Anchorage Proteins ZO-1 and ZO-3 and Impact on Drug Resistance. *Biomedicines* 2023; **11** [PMID: 38137355 DOI: 10.3390/biomedicines11123136]

37 **Li Y**, Wu L, Yong Y, Niu X, Gao Y, Zhou Q, Xie H, Liu X, Li Y, Yu Z, Abd El-Aty AM, Ju X. Enhancing gut barrier integrity: Upregulation of tight junction proteins by chitosan oligosaccharide through the ERK1/2 signaling pathway. *Nutrition* 2024; **124**: 112428 [PMID: 38663127 DOI: 10.1016/j.nut.2024.112428]

38 **Tu J**, Jiang Y, Tu L, Chen Y, Pan L, Fan X, Tian J, Li J, Wang X, Fu H, Xu B, Feng D. Da-Cheng-Qi decoction improves severe acute pancreatitis capillary leakage syndrome by regulating tight junction-associated proteins. *Front Pharmacol* 2024; **15**: 1138251 [PMID: 38708079 DOI: 10.3389/fphar.2024.1138251]

39 **Masuda D**, Nakanishi I, Ohkubo K, Ito H, Matsumoto KI, Ichikawa H, Chatatikun M, Klangbud WK, Kotepui M, Imai M, Kawakami F, Kubo M, Matsui H, Tangpong J, Ichikawa T, Ozawa T, Yen HC, St Clair DK, Indo HP, Majima HJ. Mitochondria Play Essential Roles in Intracellular Protection against Oxidative Stress-Which Molecules among the ROS Generated in the Mitochondria Can Escape the Mitochondria and Contribute to Signal Activation in Cytosol? *Biomolecules* 2024; **14** [PMID: 38275757 DOI: 10.3390/biom14010128]

Published by **Baishideng Publishing Group Inc**
7041 Koll Center Parkway, Suite 160, Pleasanton, CA 94566, USA
Telephone: +1-925-3991568
E-mail: office@baishideng.com
Help Desk: https://www.f6publishing.com/helpdesk
https://www.wjgnet.com